Tetrahedron: *Asymmetry* 19 (2008) 1288–1296

Contents lists available at ScienceDirect

Tetrahedron: *Asymmetry*

journal homepage: www.elsevier.com/locate/tetasy

Theoretical studies of stereoselectivities in the direct *anti*- and *syn*-aldol reactions catalyzed by different amino acid derivatives

Aiping Fu *, Hongliang Li, Fenghui Tian, Shuping Yuan, Hongzong Si, Yunbo Duan

Institute for Computational Science and Engineering, Laboratory of New Fiber Materials and Modern Textile, The Growing Base for State Key Laboratory, Qingdao University, Qingdao, Shandong 266071, China

ARTICLE INFO

Article history:
Received 4 April 2008
Accepted 12 May 2008
Available online 10 June 2008

ABSTRACT

Quantum mechanics calculations have been performed to study the stereoselectivities in the direct *anti*- and *syn*-aldol reactions catalyzed by different amino acid derivatives. The effects of two kinds of catalysts, L-proline amino alcohol amides and L-leucine amino alcohol amides, on the diastereoselectivity and enantioselectivity of the direct intermolecular aldol reactions between α-substituted ketones and 4-nitrobenzaldehyde have been studied. Transition states of the crucial C–C bond-forming step with the enamine intermediate addition to the aldehyde for the subject reactions are reported. These theoretical calculations provide a good explanation for the opposite *syn* versus *anti* diastereoselectivities of these two kinds of catalysts (*anti*-selectivity for the proline derivative, *syn*-selectivity for the leucine derivative). Calculated and observed diastereomeric ratios and enantiomeric excess values are in good agreement.

1. Introduction

The aldol reaction is widely regarded to be one of the most important carbon–carbon bond-formation reactions utilized in organic chemistry.[1] As a result of its usefulness for building up natural products, in particular those with polyoxygenated subunits, extensive efforts have been applied to the development of catalytic enantioselective variants of this reaction.[2] Recently, the asymmetric direct aldol reaction, which is highly atom-economic[3] compared with the well-established processes using enol or enolate derivatives as the aldol donor,[2] has received great attention, and thus many chiral catalysts including biocatalysts,[4] transition metal complexes,[5] and organocatalysts[6–8] have been discovered for this transformation. Although Shibasaki and Trost have designed bifunctional transition metal complexes for the direct catalytic asymmetric aldol reaction of aldehydes with ketones with excellent enantioselectivities,[5] catalysis of this transformation by simple metal-free organic molecules is currently receiving great interest[6–8] while organocatalysis has become a useful synthetic strategy for many important reactions. Since the pioneering finding by List et al. and Barbas et al. that L-proline could act as a catalyst in direct intermolecular aldol reactions,[6g–i] many new organocatalytic systems, which include the proline-derived *N*-sulfonylcarboxamides,[7c] L-proline amino alcohol amides,[8] and diamine-protonic acid catalysts,[7] have been developed, all attempting to reach high levels of efficiencies and to widen the scope of substrates. However, of those diastereo- and enantioselective organocatalytic direct aldol reactions, highly stereoselective strategies have been limited to *anti*-selectivity. New routes which allow high enantio- and diastereo- *syn*-selective direct aldol reactions remain an important challenge and an appealing area. Recently, Barbas et al. have developed a simple and efficient strategy to highly enantiomerically enriched *syn*-1,2-diols through direct aldol reactions involving unmodified α-hydroxyketones and 4-nitrobenzaldehyde.[9a] In these novel asymmetric aldol reactions, primary amine-containing (**PA-C**) amino acids, such as L-threonine and *O*-*t*Bu-L-threonine, were used as catalysts and the targeted *syn*-diols were obtained with high dr (up to 18:1) and ee (up to 98% ee).[9a] Later, they extended their studies on the *syn*-selective aldol reactions with protected and unprotected dihydroxyacetone by employing a series of **PA-C** amino acids as catalysts.[9b] Their interesting observations show that the **PA-C** and secondary amine-containing (**SA-C**) amino acid catalysts lead to opposite absolute configurations (*syn*-selectivity for **PA-C** and *anti*-selectivity for **SA-C** amino acids). This phenomenon can also be observed from the new type of organocatalysts developed by Gong et al.[8,10] In their previous studies,[8c] they have reported that the direct aldol reaction using a butanone donor catalyzed by proline amino alcohol amide **1A** (shown in Scheme 1) provided *anti*-selective aldol adducts with an excellent diastereomeric ratio (>99:1 dr).

* Corresponding author. Tel.: +86 532 85950767; fax: +86 532 85950768.
E-mail address: faplhl@eyou.com (A. Fu).

0957-4166/$ - see front matter © 2008 Elsevier Ltd. All rights reserved.
doi:10.1016/j.tetasy.2008.05.012

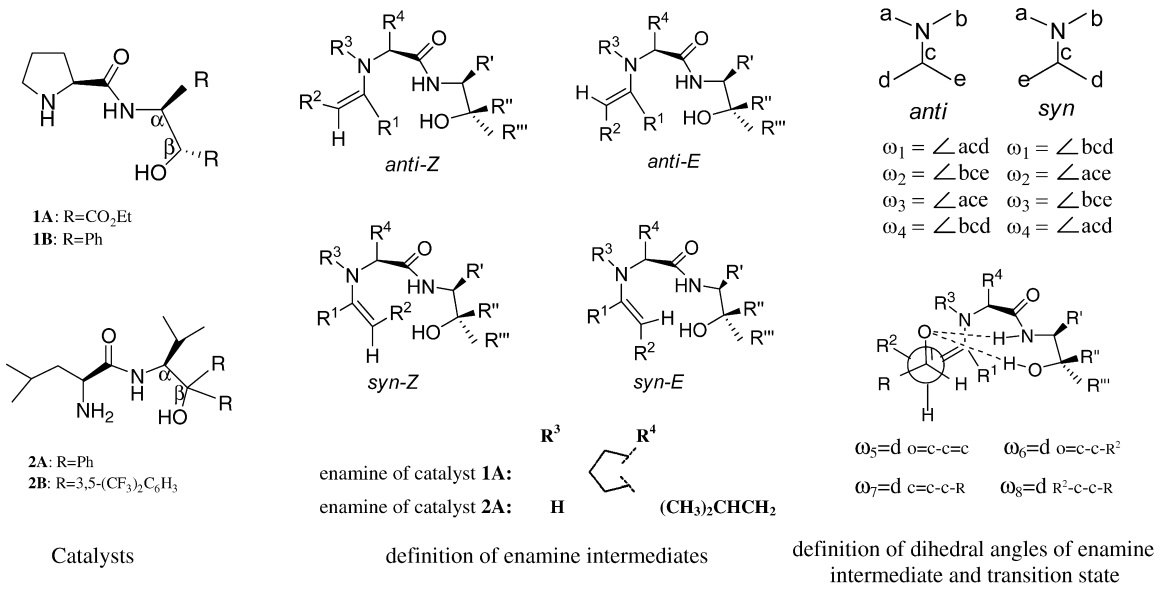

Catalysts definition of enamine intermediates definition of dihedral angles of enamine intermediate and transition state

Scheme 1.

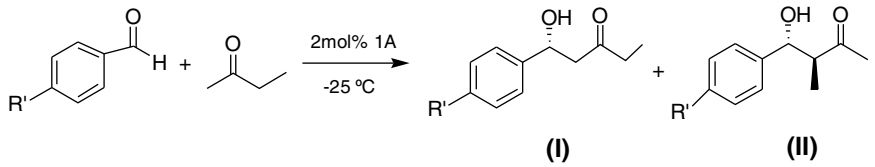

R'=NO_2	56% yield, 98%ee	42%yield, anti/syn>99:1,99%ee
R'=Cl	43% yield, 98%ee	36%yield, anti/syn>99:1,98%ee
R'=CN	62% yield, >99%ee	21%yield, anti/syn>99:1,99%ee

(1)

Recently, Gong'group has also developed a new type of organocatalysts,[10] which was derived from primary amino acids and β-amino alcohols, for the catalytic *syn*-selective direct aldol reactions of aldehydes with hydro-, fluoro-, and chloroacetone and 3-pentanone. They found that organic molecules **2A** and **2B** (shown in Scheme 1), derived from L-leucine and (*S*)-β-amino alcohols, offered superior diastereo- and enantioselectivities.

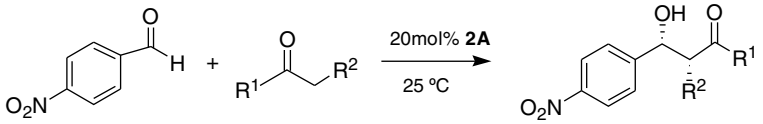

Reaction I: R^1=Me,R^2=OH, 82%~95%yield, syn/anti=5:1~19:1, 86%~96%ee
Reaction II : R^1=Me,R^2=F, 76%yield, syn/anti=5:1, 94%ee
Reaction III: R^1=Me,R^2=Cl, 81%yield, syn/anti=2.5:1, 89%ee
Reaction IV: R^1=Et,R^2=Me, 82%yield, syn/anti=4:1, 80%ee(3-$NO_2C_6H_4$ is the aldol acceptor)

(2)

These interesting observations, for example, different amino acid catalysts and their derivatives leading to opposite *syn–anti* diastereoselectivities, call for mechanistic and theoretical investigations. A number of **PA-C** and **SA-C** amino acid-catalyzed asymmetric direct aldol reactions have previously been studied by density-functional theory methods.[11–14] Pioneering theoretical and concomitant experimental studies[15] have established that the reactions proceed via enamine intermediates, while the transition states (TSs) for the crucial C–C bond-forming step (nucleophilic addition of the enamine intermediate to an electrophilically activate aldehyde) show that an arrangement of the reacting atoms is stabilized by a hydrogen-bonding interaction between the acidic proton of the carboxylic acid moiety in amino acids and the oxygen atom of the electrophile. On the basis of this concept, the diastereo- and enantioselectivities have been successfully rationalized and predicted for certain amino acids, especially proline-catalyzed intra- and intermolecular aldol reactions.

To the best of our knowledge, although great efforts have been made to explain the *anti*-selectivity of the direct aldol reactions, there are no other theoretical investigations concerning the *syn*-selectivity of the **PA-C** amino alcohol amide-catalyzed aldol reactions between α-substituted ketones and 4-nitrobenzaldehyde. Therefore, to extend our general understanding of the mechanism and stereoselectivity of the enamine catalytic reactions, the present theoretical study is performed to address the question: what is the origin of the opposite *syn*–*anti* diastereoselectivities in the **PA-C** and **SA-C** amide-catalyzed direct aldol reactions?

2. Computational methods

All ground state and transition state (TS) geometries were fully optimized using HF and B3LYP methods[16,17] at the 6-31G* basis set level. Final energies for the fully optimized structures were evaluated with the larger basis set 6-311+G** and were corrected for zero-point effects derived from frequency analysis at the corresponding HF and B3LYP/6-31G* level of theory. In some cases, the intrinsic reaction coordinate (IRC) pathways were traced in order to verify the energy profiles connecting the transition structure to the two desired minima of the proposed mechanism. Bulk effects of the solvent (acetone for Eq. 1 and reaction IV of Eq. 2, THF for reaction I of Eq. 2) on the enamine mechanism have been taken into account by means of a dielectric continuum represented by the polarizable conductor calculation model (CPCM),[18] with united-atom Kohn-Sham (UAKS) radii. The single point continuum calculations were done upon the DFT optimized gas phase geometries with a dielectric constant $\varepsilon = 20.7$ for acetone and $\varepsilon = 7.58$ for THF. All calculations were carried out using the GAUSSIAN 03 program.[19]

3. Results and discussion

To investigate the **PA-C** and **SA-C** amino acid-derived amino alcohol amide-catalyzed asymmetric direct aldol reactions involving α-substituted ketones and 4-nitrobenzaldehyde, we have used L-prolinamide derivative **1A** and L-leucinamide derivative **2A** as the protype catalysts, and Eqs. 1 and 2 (only reaction I and reaction IV in Eq. 2 were chosen) as the model reactions. Scheme 1 shows these catalysts and the notation used for the enamine intermediate and TSs.

Analogously to the previous investigation of the aldol reaction, we have focused on the TSs for the enamine attack to the aldehyde.[8a,11–14] This is expected to be the rate-determining and the stereo-controlling step of the reaction and thus to be studied in order to understand the observed diastereo- and enantioselectivities. We have considered several stereochemical pathways for this step. Firstly, enamine intermediate may in principle have a (*Z*)- or (*E*)-configuration, and the enamine double bond may be oriented *syn* and *anti* relative to the carbonyl group of the title amino acid derivatives (Scheme 1). Secondly, the different diastereomeric approach modes to the *re* and *si* faces of enamine and of the carbonyl group of the aldehyde should be considered. Consistent with the previous theoretical studies,[8a,11–14] only TSs that involve hydrogen bonding between the amide group and the terminal hydroxyl group and the aldehyde were considered here.

3.1. L-Proline amino alcohol amide-catalyzed process

Eq. 1 illustrated the *anti*-selectivity of the L-proline amino alcohol amide (catalyst **1A**)-catalyzed aldol reaction involving butanone and *para*-substituted aromatic aldehydes performed by Gong et al.[8c] The reaction preferentially occurred at the methyl group to generate product **I** in the majority and **II** in the minority. Although the regioselectivity is not significant, excellent diastereo- and enantioselectivity (dr over 99:1 in favor of *anti*-diastereomer; 98–99% ee) were obtained for the minor aldol adducts. The reaction between butanone and 4-nitrobenzaldehyde was chosen as a model to investigate the stereoselectivities addressed with catalyst **1A**.

Eight reactive channels corresponding to four stereoisomers that are *syn* and *anti*-diastereomeric pairs of enantiomers for the reaction of the C–C bond-forming step have been considered. Although the aldehyde and enamine may adopt different staggered arrangements about the forming bond, on the basis of the pioneering computational studies,[8a,11–14] only the lowest energy TSs leading to the four products have been illustrated in Figure 1. The notation used for the TSs, for example, '*anti*' and '*E*' in '*anti*-(*E*)-*re*' is consistent with previous conventions, '*re*' denotes the *re*-face of the aldehyde. The corresponding TSs occurring on the opposite sides of the proline ring that lack hydrogen-bonding stabilization are not considered. As shown in Figure 1, all the TS structures have the common features with the Gong–Wu model,[8a,b] for example, both the amide N–H and the hydroxyl groups form good hydrogen bonds with the carbonyl oxygen of the aldehyde substrate. It should be noted that the enamine derived from catalyst **1A** can rotate about the C_α–C_β bond (α,β shown in Scheme 1), and thus more TSs have to be considered. When the N–C_α–C_β–O dihedral angle is positive gauche, the two ester groups are also gauche to each other. However, when the N–C_α–C_β–O dihedral is negative gauche, the two ester groups are *anti* to each other. Our calculations confirm that TSs involving two *anti* ester groups are much more stable than their counterparts with two gauche ester groups due to the steric interactions between two ester groups in the latter case. The energy difference between the counterparts is larger than 20 kJ/mol. For simplicity, only the more stable TSs with an *anti*-conformation of two ester groups are shown in Figure 1. Furthermore, similar to the results reported by previous theoretical investigations,[8b,11–14] the TSs with *syn*-enamines are much higher in energy than those with *anti*-enamines (the energy difference between TSs involving *syn*-enamines and the most stable one **1a** is more than 35 kJ/mol), and they can be safely excluded in calculating the stereoselectivities. Therefore, only four TSs with *anti*-enamine were illustrated in Figure 1. Among these TSs, the most stable one involving the *re* attack of the *anti*-(*E*)-enamine to aldehyde **1a** leads to the (3*S*,4*R*)-enantiomer, which is consistent with the experimentally observed *anti*-aldol adduct. The other three TSs **1b**–**1d** are at least 17 kJ/mol (B3LYP/6-311+G**//HF/6-31G* level) higher in energy than **1a**. Thus, the high *anti*-diastereoselectivity (dr > 99:1) can be explained by the larger energy difference between **1a** and **1b** or **1c**. The (3*R*,4*S*)-enantiomer mainly generated from the *si* attack of *anti*-(*Z*)-enamine to aldehyde also requires a higher energy barrier (30.4 kJ/mol), which is in good agreement with the experimental results (99% ee). As shown in Figure 1, the bulk solvent has little effect on the relative energies and subsequently the stereoselectivities. Overall, whether in the gas phase or in acetone solution, there is obviously excellent agreement between the predicted and observed stereoselectivities for the L-proline amino alcohol amide-catalyzed aldol reaction.

4. L-Leucine amino alcohol amide-catalyzed process

As shown in Eq. 2, Gong et al. have also reported the *syn*-selective organocatalytic aldol reaction using hydroxy-, fluoro-, and chloroacetones and 3-pentanone as a donor to install the *syn*-aldol adducts. In their experiments, the new type of organocatalysts **2A** and **2B**, which were prepared from **PA-C** amino acids such as leucine and β-amino alcohols, offered superior diastero- and enantio-

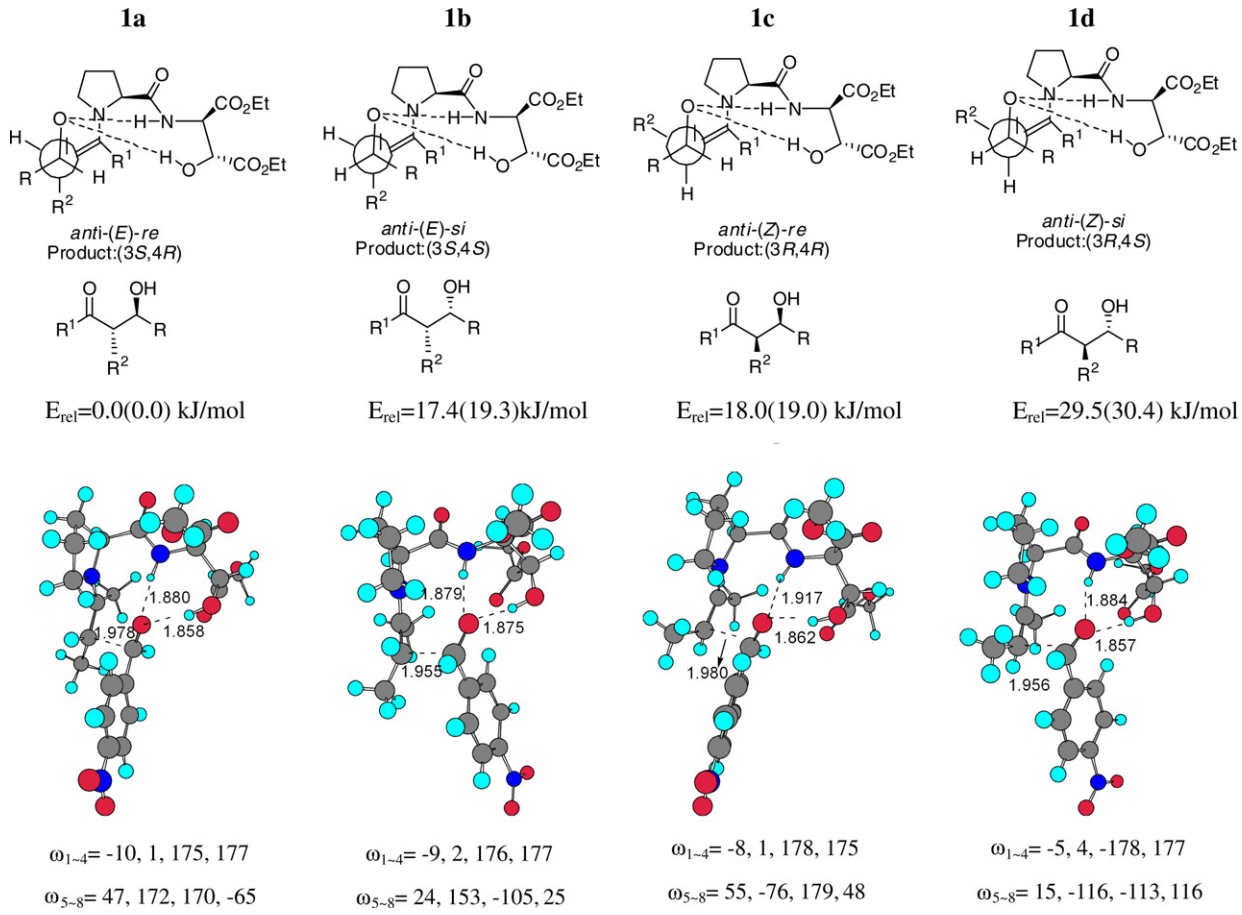

Figure 1. Transition structures and relative energies at B3LYP/6-311+G**//HF/6-31G* level including zero-point energy corrections for the reaction of the prolinamide-enamine of butanone with 4-nitrobenzyaldehyde. Values in parentheses include solvation energies in acetone using the CPCM/UAKS model at HF/6-31G* level. Different TS arrangements of aldehyde and enamine along the forming C–C bond that generate the four diastereoisomers are shown.

selectivities.[10] More importantly, compared with Barbas's first *syn*-selective works,[9a] the scope of the aldol donor is broadening, and is varied from α-hydroxyketone with the hydrogen bond donor and acceptor substituent –OH to common ketones such as 3-pentanone. These *syn*-aldol studies are based on their original explanation by transition states shown in Scheme 2: with pyrrolidine-derived catalysts **1A**, TS-I, which adopts a *Z*-enamine structure and principally generates *syn*-aldol adducts, is less favorable than TS-I′, which adopts an *E*-enamine structure and generates *anti*-aldol products, due to the steric repulsion between the R^2 group and the pyrrolidine ring in the *Z*-enamine of TS-I. While with the primary-amine-based organocatalysts such as **2A** and **2B**, the C–C bond-forming step may probably proceed via transition state TS-II′ to give *syn*-aldol products because the steric interaction between R^2 and R^3 makes TS-II, which generates an *anti*-aldol adduct, less favorable than TS-II′.

On the basis of their design considerations, we then performed density-functional theory calculations on the **2A**-catalyzed direct

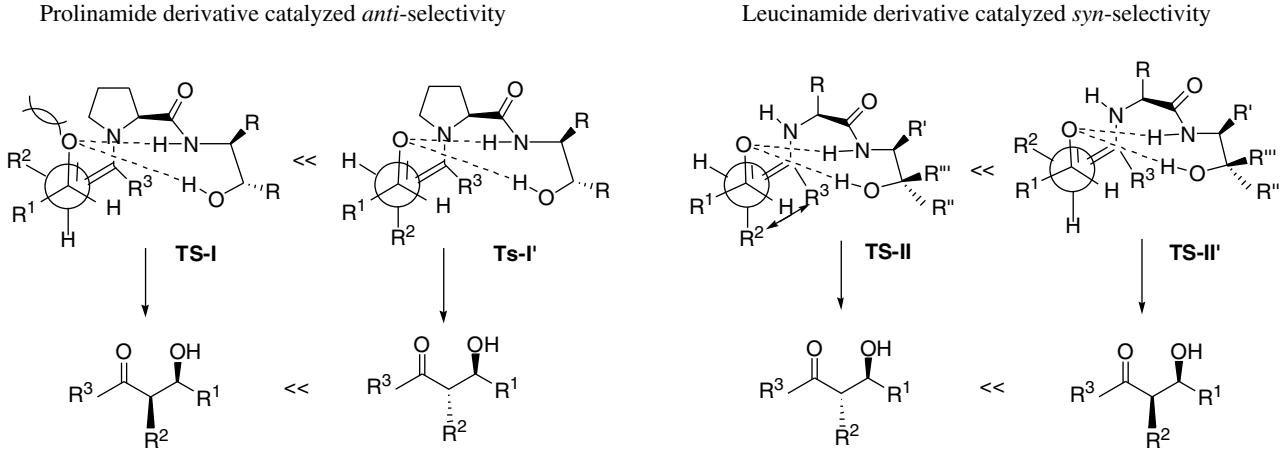

Scheme 2.

aldol reaction with hydroxyacetone and 3-pentanone as the donors and with 4-nitrobenzaldehyde as the acceptor.

Unlike the secondary cyclic amine derivative-catalyzed process, acyclic primary amine-derived enamine can rotate about the C–N bond, and thus the *E*- and *Z*-enamine are possible for both *si* and *re* attacks by the aldehyde. Therefore, more TSs have to be considered. As shown in Scheme 3, 16 TS orientations that generate four stereoisomers have been envisioned. More TSs of different arrangements of enamine and aldehyde along the forming C–C bond, which require much higher activation energies, are not discussed here. These 16 TSs can be divided into two types that differ in the attack on the opposite face of enamine interme-

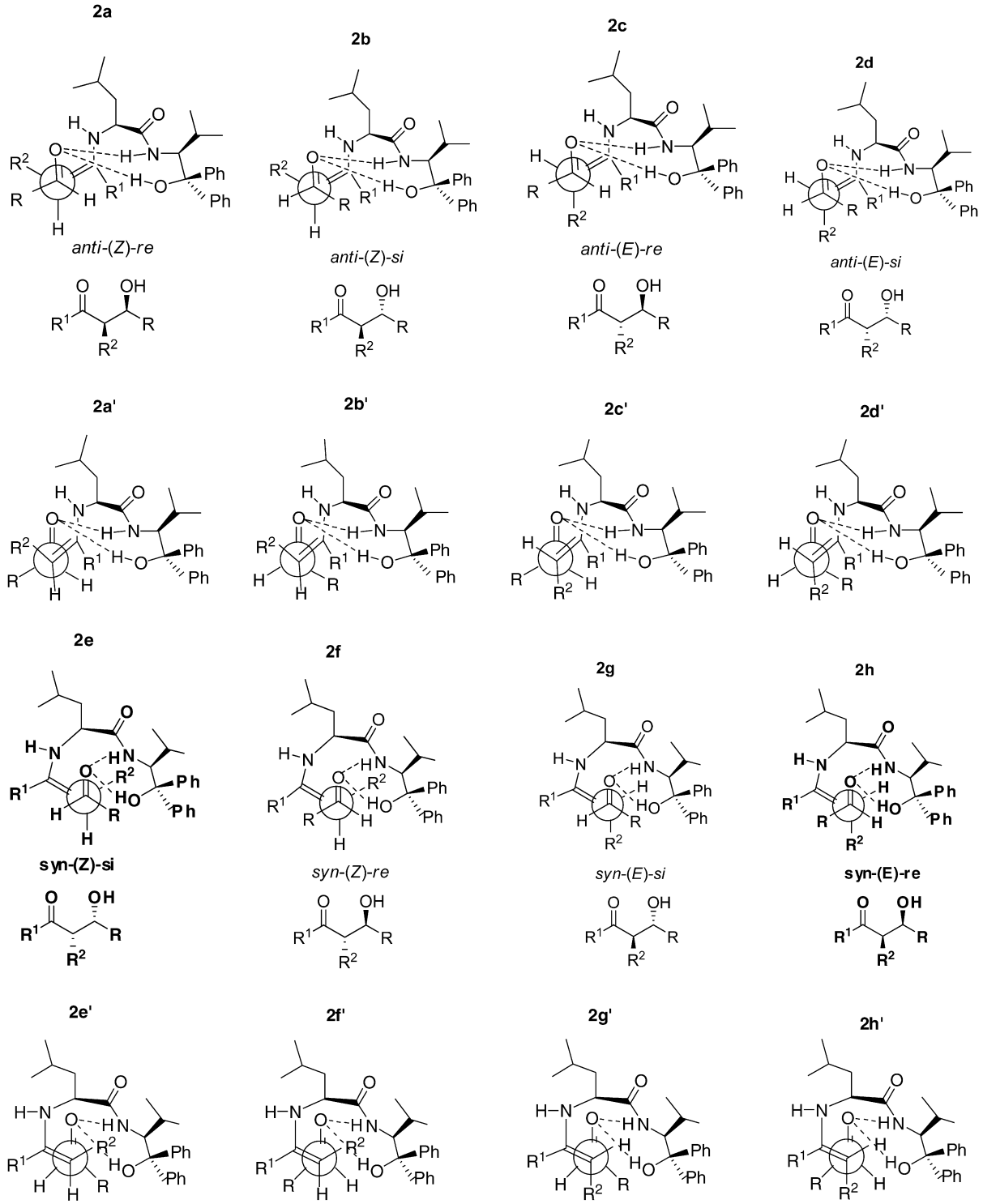

Sixteen transition state arrangements of aldehyde and leucinamide-enamine along the forming C-C bond that generate the four diastereoisomers.

Scheme 3.

diates (Type I: **2a**–**2h**, Type II: labeled by a prime, **2a**′–**2h**′), which means that products generated by transition states **2a**′-**2h**′ are enantiomers of those by TSs **2a**–**2h** correspondingly. In all cases, TSs **2a**′-**2h**′ are much higher in energy than their counterparts **2a**–**2h**, which indicates that most of these reactive channels can be safely excluded in the calculation of the stereoselectivities (**2a**′ is an exception). Among the other eight lower-energy transition states (**2a**–**2h**), similar to the results reported for proline, and its derivatives, catalyzed process,[8b,11–14] the TSs with *syn*-enamines **2e**–**2h** are higher in energy than their counterparts with *anti*-enamines **2a**–**2d**. Furthermore, in agreement with the hypothesis reported by Barbas et al.,[9a] the TSs involving (*Z*)-enamine are more stable than their counterparts involving (*E*)-enamines.

Figure 2 shows the six lower-energy TSs that generate the four different stereoisomers for the direct aldol reaction of hydroxyacetone with 4-nitrobenzaldehyde catalyzed by **2A** (reaction I in Eq. 2). Six similar TSs structures with the lower energy barriers for the reaction of 3-pentanone and 4-nitroaldehyde (reaction IV in Eq. 2) are illustrated in Figure 3. As shown in Figures 2 and 3, whether for reaction I (hydroxyacetone as the aldol donor) or reaction IV (3-pentanone as the aldol donor), the most favorable TS is **2a**, which leads to the experimentally observed major product of *syn*-selectivity. The *anti*-diastereoisomer requires a higher energy barrier (11.9 kJ/mol for reaction I and 6.8 kJ/mol for reaction IV), thus reasonably explaining the high to moderate *syn* versus *anti* diastereoselectivity from reaction I to reaction IV (dr = 19:1 for reaction I and 4:1 for reaction IV). The (3*S*,4*R*)-enantiomer is mainly formed through TS **2e** and **2a**′ for reaction I. These two TSs lie about 20 kJ/mol higher in energy than that of **2a**, which is consistent with the experimental results (96% ee). While for reaction IV, TS **2a**′ makes a large contribution to the enantioselectivity, there is somewhat overestimation over the experimental ee value. This may be due to the fact that the aldol acceptor we used in the calculation is 4-nitrobenzaldehyde, while in the experiment it was 3-nitrobenzaldehyde. However, the

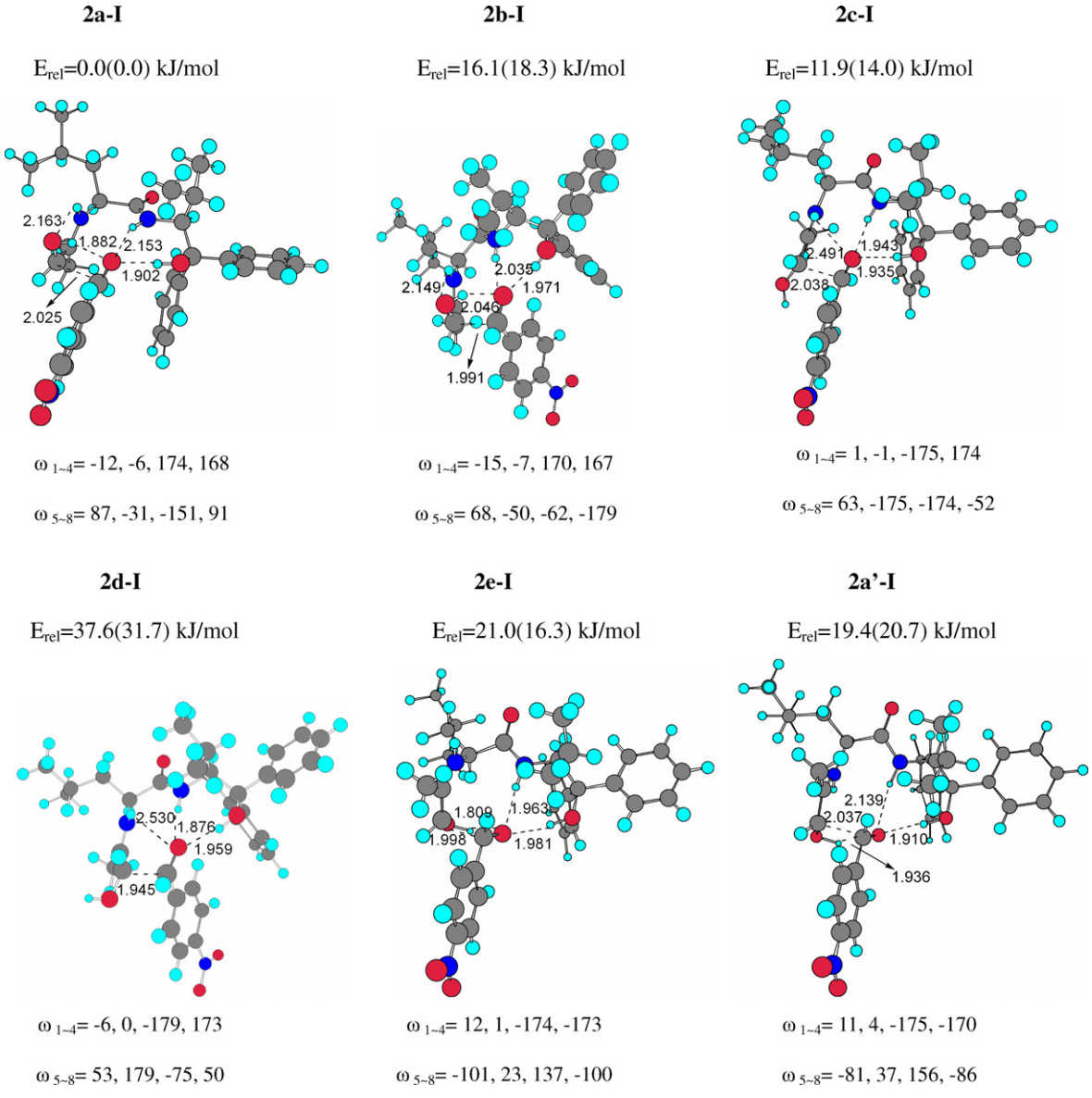

Figure 2. The more stable transition state structures and relative energies at B3LYP/6-311+G**//HF/6-31G* level including zero-point energy corrections for the reaction of the leucinamide-enamine of hydroxyacetone with 4-nitrobenzyaldehyde (reaction I in Eq. 2). Values in parentheses include solvation energies in THF using the CPCM/UAKS model at HF/6-31G* level.

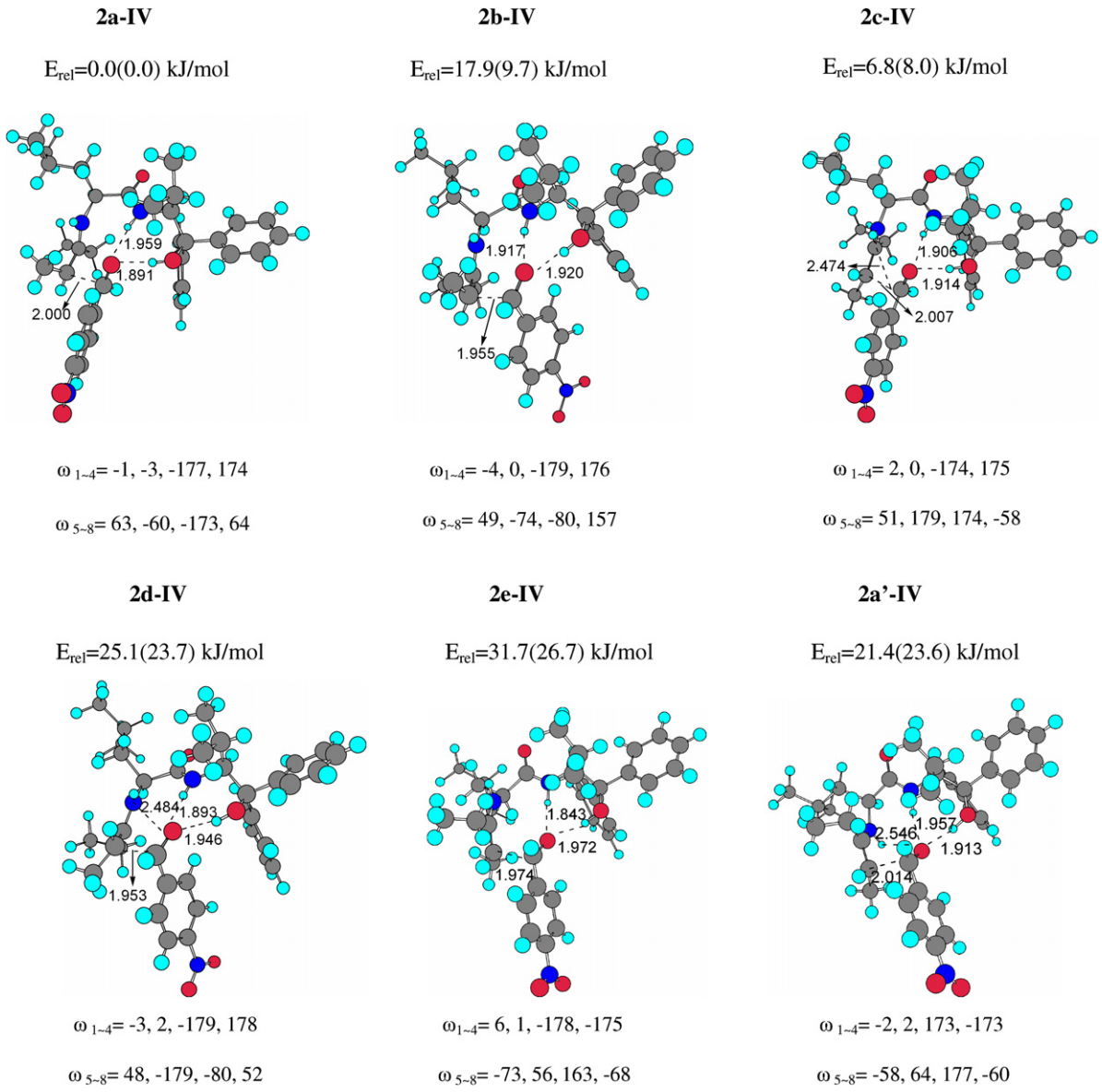

Figure 3. The more stable transition state structures and relative energies at B3LYP/6-311+G**//HF/6-31G* level including zero-point energy corrections for the reaction of the leucinamide-enamine of 3-pentanone with 4-nitrobenzyaldehyde (reaction IV in Eq. 2). Values in parentheses include solvation energies in acetone using the CPCM/UAKS model at the HF/6-31G* level.

absolute error can be tolerable and the diastereoselectivity is reproduced satisfactorily.

The origin of the opposite *syn* versus *anti* diastereoselectivities in **PA-C** and **SA-C** amino acid-catalyzed aldol reactions can be explained by scrutiny of the geometrical arrangements of the TSs (shown in Figures 1–3). Numerical values for several geometric parameters that are relevant for the relative stability of the TSs are provided in these figures. These include the lengths of the forming C–C bond and the hydrogen bond, and the distances involved in the electrostatic interactions, the dihedral angles ω_{1-4} that are commonly used to measure the deviation of the developing iminium bond from planarity (ideally 0°, 0°, 180°, and 180°, see Scheme 1), and the dihedral angles ω_{5-8} that represent the different arrangements of aldehyde and enamine along the forming C–C bond (ideally ±60° and 180° for a staggered conformation). As has been pointed out in the previous proline catalyzed aldol process,[8a,11–14] the following factors may contribute to the enantioselectivity and diastereoselectivity. First, the stereoselectivity partially arises from the different degrees to which each diastereomeric transition state satisfies iminium planarity. The more stable TS is always associated with a 'more planar' iminum moiety. The second factor that regulates the stereoselectivity is the different arrangements of the aldehyde and enamine along the forming C–C bond. Of course, intermolecular hydrogen bonding and steric repulsion may change the ideal arrangement from the staggered to the more eclipsed ones (ω_{5-8} shown in Scheme 1 and Figures 1–3). However, TSs with the more staggered orientation at the reaction center should be preferred over the other ones. The third factor arises from the different extent to which each diastereomeric TS stabilizes the forming alkoxide. On the one hand, as has been pointed out,[11,12] the favorable electrostatic interaction of $^{+\delta}$NCH$\cdots$O$^{\delta-}$ or $^{+\delta}$NH$\cdots$O$^{\delta-}$ (distances: 2.3–2.5 Å), contributes to the lower energy of the TS. On the other hand, for reaction I in Eq. 2, TSs involving the (*Z*)-enamines **2a** and **2b** are much lower in energy than their counterparts involving (*E*)-enamines **2c** and **2d**, which may be partially due to the extra hydrogen bonding provided by the OH group of the enamine to the forming alkoxide. In conclusion, these factors combine to affect the relative energies of

the various TSs and subsequently the stereoselectivity. Furthermore, despite of the above interplaying factors, when the calculated TSs for the prolinamide derivative-enamine **1a** and leucinamide derivative-enamine **2a**–**I** are compared, TS **2a**–**I** also benefits from the extra hydrogen-bonding interaction between the O atom in the OH group of the enamine and the NH group of amine. Hence, the considerable steric repulsion between the methylene substituent on the proline nitrogen atom and the methyl group in (*Z*)-enamines (in TS-**1a**) is replaced by the favorable hydrogen-bonding interaction in the counterpart of the leucinamide-catalyzed process, which makes the TSs **2a**–**I** the most stable one and consequently leads to an inversion in the diastereoselectivity. However, when the TSs of reaction IV of Eq. 2 are taken into account, we found that the existence of the extra hydrogen bond provided by the OH group of α-hydroxyketone with the NH in reaction I of Eq. 2 is not the only key point to the inversion of the diastereoselectivity. The ketone 3-pentanone, which lacks such favorable interactions, still gives rise to the major *syn*-aldol products, although an inferior diastereomeric ratio is observed. This finding indicates that the substituent groups with hydrogen bond donor and acceptor characteristics can enhance the stereochemical control, but cannot determine the inversion of the diastereoselectivity. Therefore, our calculations confirm the hypothesis by Gong et al.[10] that the opposite diastereoselectivity found with the prolinamide and leucinamide derivatives arises from the differential steric repulsion between the substituents on the enamine nitrogen (hydrogen in leucinamide, methylene in prolinamide), with the R^2 substituent of the *Z*-enamine. In the prolinamide-catalyzed aldol reaction, the steric repulsion with the methylene group destabilized the TSs involving (*Z*)-enamines, resulting in the predomination of the TS involving *anti*-(*E*)-enamines. As a consequence, the *anti*-aldol adducts is proven to be the major product. While in the leucinamide-catalyzed reactions (Scheme 2), the unfavorable steric hindrance between R^2 and R^3 destabilized the TSs involving *anti*-(*E*)-enamines and makes the TSs with *anti*-(*Z*)-enamines to be preferred. This leads to an inversion in the diastereoselectiviy as compared with that of the prolinamide-catalyzed reaction and makes the *syn*-aldol adducts to be the major product.

Table 1
Relative energies[a,b] (kJ/mol) of the more stable transition states at different levels of theory for the prolinamide derivative-catalyzed aldol reaction involving butanone and 4-nitrobenzaldehyde

	1a	1b[c]	1c	1d
HF/6-31G*	0.0	18.2	18.4	28.2
B3LYP/6-311+G**//HF/6-31G*	0.0	17.4	18.0	29.5
B3LYP/6-31G*	0.0		16.6	31.6
B3LYP/6-311+G**//B3LYP/6-31G*	0.0		17.3	29.5
CPCM//HF/6-31G*	0.0	19.3	19.0	30.4
CPCM//B3LYP/6-31G*	0.0		16.0	28.2

[a] From total energies, including zero-point vibrational energies.
[b] CPCM values including solvation energies in acetone.
[c] Transition structures for **1b** could not be obtained at B3LYP/6-31G* level.

4.1. Method and basis set effects

In order to test the effect of different methods, all of the TSs shown in Figures 1–3 were fully optimized at the HF/6-31G* and B3LYP/6-31G* levels. These two methods yield similar TSs with the forming C–C bond and the hydrogen bond distances predicted by B3LYP/6-31G* being slightly shorter than those by the HF method. The differences in the dihedral angles ω_{1-8} are very small. Tables 1 and 2 summarize the relative energies of the more stable TSs at different theory levels for **1A** and **2A**-catalyzed aldol reactions. As shown in these two tables, in most cases, the relative energies calculated by the above two methods for the structures illustrated in Figure 1–3 are close, and the stabilization order of the TSs is same. Furthermore, the single-point energy calculations for all the TSs were carried out by employing B3LYP/6-311+G** level on the HF/6-31G* and B3LYP/6-31G* optimized geometries separately to further test the validity of our lower level calculations. The results indicate that calculations with a basis set of triple zeta quality still lead to similar results to those that have been done using a basis set of only double zeta quality. Hence, even though the absolute values of the relative energies for different TSs varied with the method or basis set, it does not alter the conclusions about the stereoselectivity. Our results at the lower level of HF/6-31G* is relatively reliable for the prediction of the diastereoselectivity and enantioselectivity.

5. Conclusions

The transition structures associated with the C–C bond-formation step of the L-proline amino alcohol amide and L-leucine amino alcohol amide-catalyzed direct aldol reactions involving α-substituted ketones and 4-nitrobenzaldehyde have been studied using HF and B3LYP methods at the 6-31G* basis set level. For this stereo-controlling step, all the reactive channels corresponding to the *syn*- and *anti*-arrangement of the enamine double bond relative to the carbonyl group, and the two diastereoisomeric approach modes to the *re* and *si* faces of the carbonyl group of aldehyde, and *re* and *si* attack of leucine amino alcohol amide enamine have been studied. Our calculations confirm that the opposite *syn* versus *anti* diastereoselectivities found with the leucine derivative and the proline derivative arises from the different steric repulsion between the substituent on the enamine nitrogen (hydrogen in leucine derivative, methylene in proline derivative), with the R^2 substituent of the *Z*-enamine. The existence of the extra hydrogen bond provided by the OH group of α-hydroxyketone with the N–H can enhance the stereochemical control, but cannot determine the

Table 2
Relative energies[a,b] (kJ/mol) of the more stable transition states at different levels of theory for the leucinamide derivative-catalyzed aldol reaction involving α-hydroxyacetone and 3-pentanone with 4-nitrobenzaldehyde

	Reaction I						Reaction IV[c]					
	2a	2b	2c	2d	2e	2a′	2a	2b	2c	2d	2e	2a′
HF/6-31G*	0.0	15.6	16.2	40.0	23.5	23.0	0.0	18.5	9.9	28.7	32.8	26.0
B3LYP/6-311+G**//HF/6-31G*	0.0	16.1	11.9	37.6	21.0	19.4	0.0	17.9	6.8	25.1	31.7	21.4
B3LYP/6-31G*	0.0	14.4	19.9	47.5	21.2	22.8	0.0		6.7		30.8	20.3
B3LYP/6-311+G**// B3LYP/6-31G*	0.0	17.7	14.9	41.0	22.3	19.1	0.0		6.5		31.1	20.2
CPCM//HF/6-31G*	0.0	18.3	14.0	31.7	16.3	20.7	0.0	9.7	8.0	23.7	26.7	23.6
CPCM//B3LYP/6-31G*	0.0	17.0	19.5	33.1	13.2	20.8	0.0		5.9		22.0	18.0

[a] From total energies, including zero-point vibrational energies.
[b] CPCM values including solvation energies in THF for reaction I and acetone for reaction IV.
[c] Transition structures for **2b** and **2d** could not be obtained at B3LYP/6-31G* level.

inversion of the diastereoselectivity. The calculated diastereomeric ratios and enantiomeric excesses are in good agreement with experimental results.

Acknowledgments

This work was supported by the National Natural Science Foundation of China (Nos.: 20773071, 50602028 and 20703027). We also thank the Qingdao University Research Fund for Financial Support (063-06300506).

References

1. Kim, B. M.; Williams, S. F.; Masamune, S. In *Comprehensive Organic Synthesis*; Trost, B. M., Fleming, I., Heathcock, C. H., Eds.; Pergamon: Oxford, 1991; Vol. 2, p 229.
2. For reviews, see: (a) Gröger, H.; Vogl, E. M.; Shibasaki, M. *Chem. Eur. J.* **1998**, *4*, 1137; (b) Nelson, S. G. *Tetrahedron: Asymmetry* **1998**, *9*, 357; (c) Carreira, E. M.. In *Comprehensive Asymmetric Catalysis*; Jacobsen, E. N., Pfaltz, A., Yamamoto, H., Eds.; Springer: Heidelberg, 1999; Vol. III. Chapter 29.1 (d) Mahrwald, R. *Chem. Rev*. **1999**, *99*, 1095; (e) Machajewski, T. D.; Wong, C.-H. *Angew. Chem., Int. Ed.* **2000**, *39*, 1352; (f) Johnson, J. S.; Evans, D. A. *Acc. Chem. Res.* **2000**, *33*, 325; (g) Denmark, S. E.; Stavenger, R. A. *Acc. Chem. Res.* **2000**, *33*, 432; (h) Palomo, C.; Oiarbide, M.; García, J. M. *Chem. Soc. Rev.* **2004**, *33*, 65.
3. (a) Trost, B. M. *Science* **1991**, *254*, 1471; (b) Trost, B. M. *Angew. Chem., Int. Ed. Engl.* **1995**, *34*, 259.
4. (a) Barbas, C. F., III; Heine, A.; Zhong, G.; Hoffmann, T.; Gramatikova, S.; Björnestedt, R.; List, B.; Anderson, J.; Stura, E. A.; Wilson, I. A.; Lerner, R. A. *Science* **1997**, *278*, 2085; (b) Hoffmann, T.; Zhong, G.; List, B.; Shabat, D.; Anderson, J.; Gramatikova, S.; Lerner, R. A.; Barbas, C. F., III. *J. Am. Chem. Soc.* **1998**, *120*, 2768; (c) List, B.; Shabat, D.; Barbas, C. F., III; Lerner, R. A. *Chem. Eur. J.* **1998**, *4*, 881.
5. (a) Yamada, Y. M. A.; Yoshikawa, N.; Sasai, H.; Shibasaki, M. *Angew. Chem., Int. Ed.* **1997**, *36*, 1871; (b) Yoshikawa, N.; Yamada, Y. M. A.; Sasai, H.; Shibasaki, M. *J. Am. Chem. Soc.* **1999**, *121*, 4168; (c) Trost, B. M.; Ito, H. *J. Am. Chem. Soc.* **2000**, *122*, 12003; (d) Trost, B. M.; Ito, H.; Siloff, E. R. *J. Am. Chem. Soc.* **2001**, *123*, 3367; (e) Evans, D. A.; Downey, C. W.; Hubbs, J. L. *J. Am. Chem. Soc.* **2003**, *125*, 8706.
6. For reviews, see: (a) List, B. *Tetrahedron* **2002**, *58*, 5573; (b) List, B. *Acc. Chem. Res.* **2004**, *37*, 548; (c) Notz, W.; Tanaka, F.; Barbas, C. F., III. *Acc. Chem. Res.* **2004**, *37*, 580; (d) Dalko, P. I.; Moisan, L. *Angew. Chem., Int. Ed.* **2004**, *43*, 5138; For pioneering works. see: (e) Hajos, Z. G.; Parrish, D. R. *J. Org. Chem.* **1974**, *39*, 1615; (f) Eder, U.; Sauer, G.; Wiechert, R. *Angew. Chem., Int. Ed. Engl.* **1971**, *10*, 496; (g) List, B.; Lerner, R. A.; Barbas, C. F., III. *J. Am. Chem. Soc.* **2000**, *122*, 2395; (h) Sakthivel, K.; Notz, W.; Bui, T.; Barbas, C. F., III. *J. Am. Chem. Soc.* **2001**, *123*, 5260; (i) Notz, W.; List, B. *J. Am. Chem. Soc.* **2000**, *122*, 7386; (j) Northrup, A. B.; MacMillan, D. W. C. *J. Am. Chem. Soc.* **2002**, *124*, 6798; (k) Bøgevig, A.; Kumaragurubaran, N.; Jørgensen, K. A. *Chem. Commun.* **2002**, 620; (l) Casas, J.; Engqvist, M.; Ibrahem, I.; Kaynak, B.; Córdova, A. *Angew. Chem., Int. Ed.* **2005**, *44*, 1343.
7. (a) Hartikka, A.; Arvidsson, P. I. *Tetrahedron: Asymmetry* **2004**, *15*, 1831; (b) Torii, H.; Nakadai, M.; Ishihara, K.; Saito, S.; Yamamoto, H. *Angew. Chem., Int. Ed.* **2004**, *43*, 1983; (c) Berkessel, A.; Koch, B.; Lex, J. *Adv. Synth. Catal* **2004**, *346*, 1141; For a review, see: (d) Saito, S.; Yamamoto, H. *Acc. Chem. Res.* **2004**, *37*, 570.
8. (a) Tang, Z.; Jiang, F.; Yu, L.-T.; Cui, X.; Gong, L.-Z.; Mi, A.-Q.; Jiang, Y.-Z.; Wu, Y.-D. *J. Am. Chem. Soc.* **2003**, *125*, 5262; (b) Tang, Z.; Jiang, F.; Cui, X.; Gong, L.-Z.; Mi, A.-Q.; Jiang, Y.-Z.; Wu, Y.-D. *Proc. Natl. Acad. Sci. U.S.A.* **2004**, *101*, 5755; (c) Tang, Z.; Yang, Z.-H.; Chen, X.-H.; Cun, L.-F.; Mi, A.-Q.; Jiang, Y.-Z.; Gong, L.-Z. *J. Am. Chem. Soc.* **2005**, *127*, 9285.
9. (a) Ramasastry, S. S. V.; Zhang, H.; Tanaka, F.; Barbas, C. F., III. *J. Am. Chem. Soc.* **2007**, *129*, 288; (b) Ramasastry, S. S. V.; Albertshofer, K.; Utsumi, N.; Tanaka, F.; Barbas, C. F., III *Angew. Chem., Int. Ed.* **2007**, *46*, 5572.
10. Xu, X. Y.; Wang, Y. Z.; Gong, L. Z. *Org. Lett.* **2007**, *9*, 4247.
11. (a) Bahmanyar, S.; Houk, K. N. *J. Am. Chem. Soc.* **2001**, *123*, 11273; (b) Bahmanyar, S.; Houk, K. N. *J. Am. Chem. Soc.* **2001**, *123*, 12911; (c) Bahmanyar, S.; Houk, K. N.; Martin, H. J.; List, B. *J. Am. Chem. Soc.* **2003**, *125*, 2475; (d) Allemann, C.; Gordillo, R.; Clemente, F. R.; Cheong, P. H.; Houk, K. N. *Acc. Chem. Res.* **2004**, *37*, 558; (e) Clemente, F. R.; Houk, K. N. *Angew. Chem., Int. Ed.* **2004**, *43*, 5766; (f) Clemente, F. R.; Houk, K. N. *J. Am. Chem. Soc.* **2005**, *127*, 11294; (g) Cheong, P. H.; Houk, K. N.; Warrier, J. S.; Hanessian, S. *Adv. Synth. Catal.* **2004**, *346*, 1111.
12. Rankin, K. N.; Gauld, J. W.; Boyd, R. J. *J. Phys. Chem. A* **2002**, *106*, 5155.
13. (a) Arno, M.; Domingo, L. R. *Theor. Chem. Acc.* **2002**, *108*, 232; (b) Arno, M.; Zaragoza, R. J.; Domingo, L. R. *Tetrahedron: Asymmetry* **2005**, *16*, 2764.
14. Bassan, A.; Zou, W.; Reyes, E.; Himo, F.; Cordova, A. *Angew. Chem., Int. Ed.* **2005**, *44*, 7028.
15. (a) Hoang, L.; Bahmanyar, S.; Houk, K. N.; List, B. *J. Am. Chem. Soc.* **2003**, *125*, 16; (b) List, B.; Hoang, L.; Martin, H. J. *Proc. Natl. Acad. Sci. U.S.A.* **2004**, *101*, 5839.
16. (a) Becke, A. D. *J. Chem. Phys.* **1993**, *98*, 1372–1377; (b) Becke, A. D. *J. Chem. Phys.* **1993**, *98*, 5648–5652; (c) Becke, A. D. *Phys. Rev. A* **1988**, *38*, 3098–3100.
17. Lee, C.; Yang, W.; Parr, R. G. *Phys. Rev. B* **1988**, *37*, 785–789.
18. (a) Barone, V.; Cossi, M. *J. Phys. Chem. A* **1998**, *102*, 1995; (b) Barone, B.; Cossi, M.; Tomasi, J. *J. Comput. Chem.* **1998**, *19*, 404.
19. Frisch, M. J.; Trucks, G. W.; Schlegel, H. B.; Scuseria, G. E.; Robb, M. A.; Cheeseman, J. R.; Montgomery, J. A., Jr.; Vreven, T.; Kudin, K. N.; Burant, J. C.; Millam, J. M.; Iyengar, S. S.; Tomasi, J.; Barone, V.; Mennucci, B.; Cossi, M.; Scalmani, G.; Rega, N.; Petersson, G. A.; Nakatsuji, H.; Hada, M.; Ehara, M.; Toyota, K.; Fukuda, R.; Hasegawa, J.; Ishida, M.; Nakajima, T.; Honda, Y.; Kitao, O.; Nakai, H.; Klene, M.; Li, X.; Knox, J. E.; Hratchian, H. P.; Cross, J. B.; Adamo, C.; Jaramillo, J.; Gomperts, R.; Stratmann, R. E.; Yazyev, O.; Austin, A. J.; Cammi, R.; Pomelli, C.; Ochterski, J. W.; Ayala, P. Y.; Morokuma, K.; Voth, G. A.; Salvador, P.; Dannenberg, J. J.; Zakrzewski, V. G.; Dapprich, S.; Daniels, A. D.; Strain, M. C.; Farkas, O.; Malick, D. K.; Rabuck, A. D.; Raghavachari, K.; Foresman, J. B.; Ortiz, J. V.; Cui, Q.; Baboul, A. G.; Clifford, S.; Cioslowski, J.; Stefanov, B. B.; Liu, G.; Liashenko, A.; Piskorz, P.; Komaromi, I.; Martin, I. L.; Fox, D. J.; Keith, T.; Al-Laham, M. A.; Peng, C. Y.; Nanayakkara, A.; Challacombe, M.; Gill, P. M. W.; Johnson, B.; Chen, W.; Wong, M. W.; Gonzales, C.; Pople, J. A. GAUSSIAN *03, Revision D.01*; Gaussian: Wallingford, CT, 2004.